Semicond. Sci. Technol. 9 (1994) 2031–2041. Printed in the UK

Scattering of a two-dimensional electron gas by a correlated system of ionized donors

E Buks, M Heiblum, Y Levinson and Hadas Shtrikman

Braun Center for Sub Micron Research, Department of Condensed Matter Physics, Weizmann Institute of Science, Rehovot 76100, Israel

Received 14 June 1994, accepted for publication 14 July 1994

Abstract. Using selectivity doped GaAs–AlGaAs heterostructures we provide conclusive evidence that correlation among the DX^{-}–d^{+} charged donors strongly enhances the mobility of a two-dimensional electron gas (2DEG) residing 10 nm away from the charged donors. This is accomplished by changing the extent of correlation without affecting the total number of charged donors and density of electrons in the 2DEG. The experiments are used to prove that the DX donors are negatively charged in their ground state. A theory treating correlated DX^{-}–d^{+} charges can approximately account for these results.

1. Introduction

A selectively doped GaAs–AlGaAs heterostructure, supporting a two-dimensional electron gas (2DEG), enables high-mobility transport of electrons in pure GaAs. This is because the parent donors, situated in $Al_xGa_{1-x}As$, are spatially separated from the undoped GaAs by an undoped $Al_xGa_{1-x}As$ spacer [1,2]. As long as the width of the spacer does not exceed some 50 nm the low-temperature mobility is usually limited by the parent donor impurities [1], leading to long-range, small-angle, scattering. Consequently, the momentum relaxation time, τ_t, representing the rate of momentum randomization, is longer than the single-particle relaxation time, τ_s, associated with the quantum state lifetime [3]. Under the assumption that the ionized donors are randomly distributed one obtains $1/\tau_s$, $1/\tau_t \propto n_0$, with n_0 being the density of ionized donors [4]. A comparison with experiments generally reveals that the scattering times are underestimated by this approach. If, however, the charged impurities were to be correlated due to their mutual Coulombic interaction, the expected scattering times could be substantially higher (in 2D systems: [5–14]; in 3D systems: [15–22]), explaining this discrepancy. Moreover, these types of heterostructures are ideal systems to identify possible charge correlation among the randomly distributed donor atoms because of the relative ease in changing the net charge of the donor layer, the extent of donor correlation and the density of the electrons in the 2DEG all in the same device.

According to the recently proposed negative-U model [23,24], any isolated group IV donor in a III–V compound semiconductor can be in one of two different configurations: a hydrogenic-like, shallow donor (d^{+}, d^{0}) at a substitutional site, and a DX-like, deep metastable donor at an interstitial site. The latter is associated with the donor atom displaced along the ⟨111⟩ direction, leaving a vacancy at the substitutional site [25]. In Si-doped $Al_xGa_{1-x}As$ alloy, the DX level, which is degenerate with the conduction band in GaAs, moves into the gap for $x > 0.2$. With increased AlAs mole fraction a few different donor levels develop, and each is related to the number of Al atoms near the displaced Si atom [26]. As the AlAs mole fraction is increased all energy levels follow approximately the L band position, with the lowest of them having a maximal activation energy of some 160 meV around $x \simeq 0.37$, corresponding to the direct (Γ) to indirect (X) crossover point [26]. Although it is not accurately determined yet, all levels seem to merge with the indirect, X, conduction band near $x = 0.8$. The metastability of the DX centres is exhibited mainly by the persistence of their charge below some freeze-out temperature (about 130 K for Si DX for $x = 0.37$). This persistence effect can be explained in terms of repulsive configurational (electronic–elastic) barriers for emission and capture of electrons between (deep) DX centres and shallow levels. As long as the thermal energy is small compared to the height of these configurational-type repulsive barriers the emission and capture of electrons are negligibly small and the sample remains in a non-equilibrium state.

To study the effect of correlation we first verify that the charge state of the metastable DX-like Si atoms, in their ground state, is negative; thus agreeing with the negative-U model [23,24]. Then, we exploit the DX metastability to control the net charge within the donor layer electrostatically (by applying a gate voltage while

0268-1242/94/112031+11$19.50 © 1994 IOP Publishing Ltd

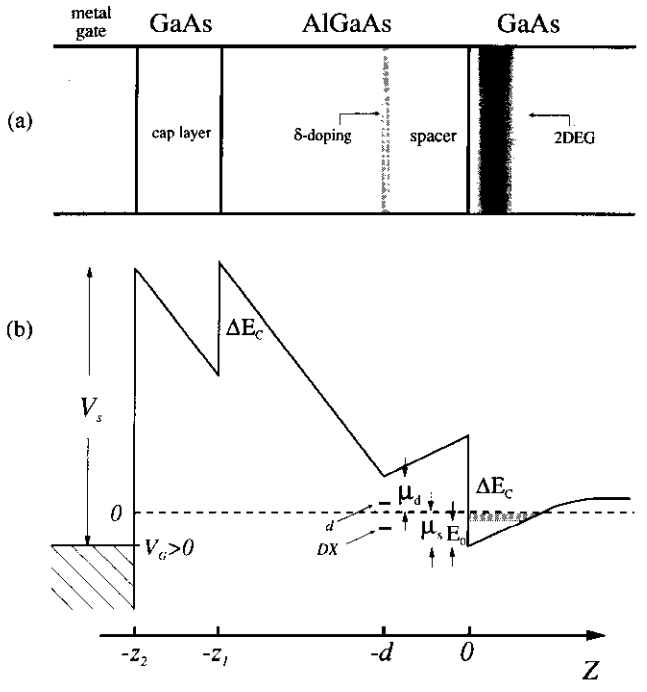

Figure 1. (*a*) Layer configuration of a δ-doped heterostructure supporting a 2DEG. (*b*) Energy band diagram of the heterostructure with gate bias $V_G > 0$. The two relevant donor levels are d and DX, and μ_d is the chemical potential associated with the donor system.

cooling the sample), and then freeze it during the cooling process. This enables us to compare the low-temperature mobility (serving as a sensor for charge correlation) for different ratios of $n(d^+)/n(DX^-)$ (where $n(d)$ stands for the density of the corresponding donors) but for the same electron density, the same density of scatterers and in the same device. Doing so, we find an enhancement in the mobility of the 2DEG by at least a factor of six. We can account for these results by modifying the more standard mobility calculations to correct for correlation among the charged donors.

Several heterostructures of GaAs–$Al_{0.37}Ga_{0.63}As$ and GaAs–AlAs were grown by molecular beam epitaxy (MBE) on (100)-oriented semi-insulating GaAs substrates. In these structures electrons are supplied to the 2DEG via δ-doping of Si in the AlGaAs layer, namely, a plane layer of Si doping [27] separated from the 2DEG by an undoped AlGaAs spacer (figure 1). The spacer width was chosen to be only 10 nm in order to ensure that scattering at low temperatures is dominated by the ionized donors in the δ-doping plane [1]. Growth was performed at a low substrate temperature in order to minimize Si diffusing out of the δ plane. Gated Hall bars were fabricated by a conventional photolithographical process. In order to minimize mobility degradation resulting from fast electrons and soft x-rays, which are normally produced during electron beam evaporation [28], the metal gates were deposited by thermal evaporation. The mobility, single-particle scattering rate and density of the 2DEG were measured via Hall and Shubnikov–de Haas (SdH) measurements.

In what follows we describe the nature of freeze-out of the DX centres and its effect on the density of the 2DEG (section 2), this is followed by measurements of the mobility under different conditions in order to monitor the effect of correlation among charged donors (section 3). The observed effects of correlation are then discussed theoretically and comparison with the experiments is given (sections 4 and 5).

2. Donor freeze-out and their charge states

In this section we present the consequence of the gradual freeze-out process of the DX centres. Our results allow finding the energies associated with the donor levels (section 2.1) and the frozen net charge in the δ-doping plane (section 2.2). The experiments are carried out with a GaAs–$Al_{0.37}Ga_{0.63}As$ heterostructure having a spacer width $d = 10$ nm and Si concentration of 7.5×10^{12} cm^{-2} (see figure 1). Comparisons with other samples will be presented in section 3.4.

2.1. Freeze-out of DX centres

The metastable nature of DX centres can be studied via measurements of the density of the 2DEG, n_s, at a temperature, T_m, in the vicinity of freeze-out. The density measured via Hall and SdH measurements as a function of gate voltage, V_G, and temperature, T_m, is plotted in figure 2(*a*). Note that before each measurement the sample was cooled down from above 200 K to T_m, while zero gate voltage was applied. For $T_m \geqslant 160$ K the density of the 2DEG is approximately constant over a wide range of V_G (limited by gate leakage currents), indicating that the Fermi level is pinned (most likely to a donor level). For $T_m < 160$ K the $n_s(V_G)$ curves exhibit a different behaviour, consisting of a saturation regime at high V_G—consistent with a pinned Fermi level—and a linear regime at lower V_G—indicating a constant gate–2DEG capacitance. The linear regime indicates that active (unfrozen) donor levels are empty and the total charge within the δ-doping plane does not change with V_G.

Assuming that the saturation of n_s at different temperatures is associated with pinning of the Fermi level to a particular donor state, the corresponding energy of the donor state can be obtained by

$$\mu_d = \Delta E_c - eF_z(0^-)d - \mu_s \qquad (2.1)$$

where, as shown in figure 1, ΔE_c is the conduction band discontinuity between GaAs and $Al_xGa_{1-x}As$ and F_z is the z component of the electric field. A single integration of Poisson equation from $z = 0^+$ to $+\infty$, where $F_z(+\infty) = 0$, neglecting the charge of the unintentional ionized impurities in the GaAs (depletion charge, n_{depl})† yields: $F_z(0^+) = en_s/\varepsilon_1\varepsilon_0$, where $\varepsilon_1(\varepsilon_2)$ is the dielectric constant of GaAs ($Al_xGa_{1-x}As$). The

† The depletion charge is given approximately by [1]: $n_{depl} = (2\varepsilon\varepsilon_0 E_g n_A/e^2)^{1/2}$ where E_g is the energy gap of GaAs and n_A is the net acceptor concentration. For the background doping level in our MBE system $n_{depl} < 5 \times 10^{10}$ cm^{-2}.

boundary conditions at the interface $z = 0$ yield $\varepsilon_1 F_z(0^+) = \varepsilon_2 F_z(0^-)$, leading to

$$F_z(0^-) = \frac{en_s}{\varepsilon_2 \varepsilon_0}. \tag{2.2}$$

Within the effective mass approximation the energy spectrum of the 2DEG is given by

$$E_{k,i} = \frac{\hbar^2 k^2}{2m^*} + E_i \tag{2.3}$$

where m^* is the effective mass of the electrons, k is the magnitude of the wavevector associated with the free motion in the plane and the set E_i $(i \geqslant 0)$ are the energy levels associated with motion in the z direction of the triangular-like quantum well near the interface $z = 0$. Since the allowed values of k are uniformly distributed in the phase plane with a density given by $L^2/2\pi^2$ (L^2 is the area of the 2DEG), the density of k states per unit area associated with this energy spectrum is constant for each subband and is given by

$$D(E) = D_0 \sum_i \theta(E - E_i) \tag{2.4}$$

where E is the energy, $D_0 = m^*/\pi\hbar^2$, and θ is the Heaviside function (the step function). Using $D(E)$, the areal density, n_s, can be obtained with Fermi–Dirac statistics

$$n_s = \int D(E) \frac{\mathrm{d}E}{1 + \exp[\beta(E - \mu_s)]} \tag{2.5}$$

with $\beta = 1/k_B T$. Thus, n_s is given by

$$n_s = \frac{D_0}{\beta} \sum_i \ln\{1 + \exp[\beta(\mu_s - E_i)]\}. \tag{2.6}$$

Since, in our case, only the ground state, E_0, of the quantum well is occupied, one obtains

$$\mu_s - E_0 = \frac{1}{\beta} \ln\left[\exp\left(\frac{n_s \beta}{D_0}\right) - 1\right] \tag{2.7}$$

where E_0 can be estimated by the Fang–Howard approximation [1]

$$E_0 = \left(\frac{3}{2}\right)^{5/3} \left(\frac{e^2\hbar}{\sqrt{m^*}\varepsilon_1\varepsilon_0}\right)^{2/3} \frac{n_{\mathrm{depl}} + (55/96)n_s}{[n_{\mathrm{depl}} + (11/32)n_s]^{1/3}}. \tag{2.8}$$

When equation (2.1) is combined with equations (2.2), (2.7) and (2.8) one obtains the chemical potential, μ_d, as a function of the density of the 2DEG, n_s.

In figure 2(b), the plotted chemical potential, μ_d, as a function of T_m is derived from the saturated density of the 2DEG using equation (2.1). As the sample is being cooled, lower-lying states freeze out and only higher donor levels remain active. The Fermi level thus climbs, pinning itself approximately to the lowest active state. Our results suggest that the DX energy levels lie in the range of 120 meV to 155 meV (owing to the finite temperature the levels position is not absolutely certain), and they gradually freeze out as the temperature is decreased from 150 K to 120 K. Moreover, below a temperature of 120 K the lowest active donor level is some 90 meV deep, substantially higher than the deepest DX donor level, but with a binding energy considerably larger than that expected from a hydrogenic-like level associated with Γ or X conduction band valleys. This active donor level might be the often mentioned A_1 level [26].

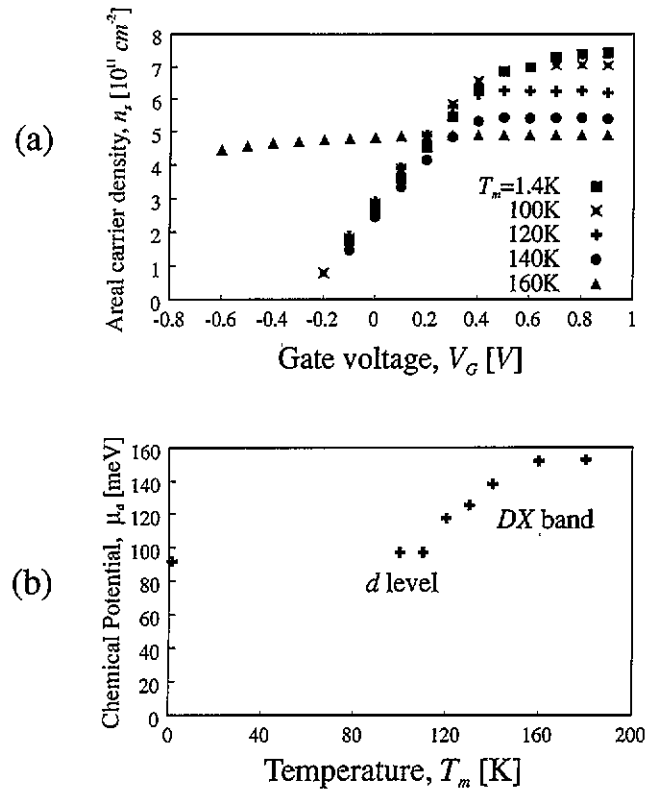

Figure 2. (a) The areal carrier density versus gate voltage at various temperatures. (b) The chemical potential, μ_d, versus temperature, calculated by equation (2.1) from the density of the 2DEG.

The gradual nature of the freeze-out process can be explained by the multiplicity of DX levels. The lattice distortion, associated with a creation of a DX centre, results in a displacement of the Si atom along the ⟨111⟩ direction. Consequently, the displaced Si atom has three different configurations of the column III atoms as close neighbours. In GaAs there is only one possible configuration where all column III nearest neighbours are Ga atoms and the DX configuration is unique. In the $Al_xGa_{1-x}As$ alloy, however, there are four possible configurations, related to 0, 1, 2 and 3 Al atoms near the displaced Si atom; each resulting in a different donor activation energy. It turns out that these four different levels span the interval 120–155 meV for an AlAs mole fraction of $x = 0.37$.

2.2. Net frozen charge in the δ-doping plane

The metastable nature of the DX centres enables us to change the population of the DX donors in the δ-doping plane. This can be attained by applying a gate voltage,

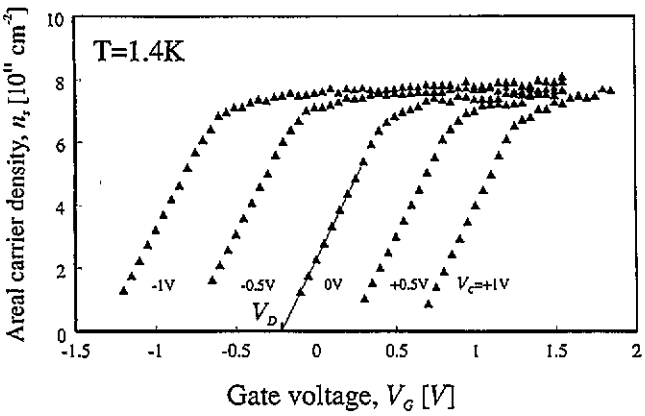

Figure 3. Areal carrier density in the 2DEG versus gate voltage for several thermal cycles with different values of cooling gate voltages, V_C. In the linear regime the charge in the donor layer is constant and in the saturation regime the gate is screened. V_D is the depletion voltage, namely $n_s(V_D) = 0$, for a particular thermal cycle.

V_C, at temperatures above the freeze-out temperature, T_f, and keeping it constant as we cool the sample to a temperature below 120 K, thus freezing the donor configuration. For relatively large V_Cs (more positive), more electrons populate the donors and the chemical potential of the donor system, μ_d, becomes smaller (see figure 1); for smaller V_Cs the opposite occurs. When the sample is already at low temperatures, the gate voltage, to be named V_G, can be varied, thus changing the concentration of the 2DEG without affecting the frozen concentration of the DX centres determined only by V_C. This procedure is being named thermal cycle.

The results of a few thermal cycles are seen in figure 3. We plot the density of the 2DEG, n_s, versus the gate voltage, V_G. All branches (for different V_Cs) have a similar structure, consisting of a linear regime at relatively low V_G and a saturation regime at a higher V_G. As before, the linear regime indicates a fixed gate–2DEG capacitance, while the saturation regime is a manifestation of electrons flooding the shallower d^+ active donor sites, thus screening the field of the gate. In other words, the transition to the saturation regime occurs when the Fermi level reaches the lowest active level, d^0, and as long as this level is not completely filled it is pinned to it—preventing a further increase in the density of the 2DEG with increasing V_G.

The fixed donor charge density within each of the linear regimes seen in figure 3, ρ_0, determined by the cooling gate voltage, V_C, strongly affects the transport properties of the 2DEG. Its value can be calculated in two ways:

(i) using the Poisson equation, the measured depletion voltage, V_D (V_D is defined so that $n_s(V_D) = 0$, as seen in figure 3) and the structure parameters (section 2.2.1); and

(ii) using level statistics and μ_d obtained before (section 2.2.2).

The comparison between the two methods of calculation enables us to determine the charge state of the DX centres in the ground state (section 2.2.3). As this is a controversial issue the charge state will be reconfirmed from mobility measurements described in section 3.1.

2.2.1. Net charge determined using the Poisson equation. As seen in figure 1 the following relation holds

$$\Delta E_c + e[V(-z_2) - V(0^-)] = e(V_S - V_G) + \mu_s \quad (2.9)$$

where, in addition to the known parameters, V_S is the Schottky barrier voltage at the metal–semiconductor interface and $V(z)$ is the potential along the growth direction. In turn, the one-dimensional potential can be determined from the Poisson equation

$$\frac{\partial^2 V(z)}{\partial z^2} = -\frac{q(z)}{\varepsilon_0 \varepsilon(z)} \quad (2.10)$$

with $q(z)$ being the 3D charge density and $\varepsilon_0\varepsilon(z)$ the local dielectric constant. By integrating the Poisson equation twice we find

$$V(-z_2) - V(0^-) = -F_z(0^-)\left(z_1 + \frac{\varepsilon_2}{\varepsilon_1}(z_2 - z_1)\right) + \frac{\rho_0}{e\varepsilon_2\varepsilon_0}\left(z_1 - d + \frac{\varepsilon_2}{\varepsilon_1}(z_2 - z_1)\right) - \frac{\Delta E_c}{e}.$$

The term μ_s in equation (2.9) (which is estimated in section 2.1) can be neglected compared with all other terms (in particular for low n_s, in the vicinity of V_D), and thus

$$en_s = C_{2DEG}(V_G - V_D) \quad (2.11)$$

where C_{2DEG} is the capacitance between the gate and the 2DEG

$$C_{2DEG}^{-1} = C_1^{-1} + C_2^{-1} = \left(\frac{e\varepsilon_0\varepsilon_1}{z_2 - z_1}\right)^{-1} + \left(\frac{e\varepsilon_0\varepsilon_2}{z_1}\right)^{-1} \quad (2.12)$$

and the net donor charge 2D density is

$$\rho_0 = C_\delta(V_S - V_D). \quad (2.13)$$

where C_δ is the capacitance between the gate and the δ-doping layer

$$C_\delta^{-1} = C_1^{-1} + C_3^{-1} = \left(\frac{e\varepsilon_0\varepsilon_1}{z_2 - z_1}\right)^{-1} + \left(\frac{e\varepsilon_0\varepsilon_2}{z_1 - d}\right)^{-1}. \quad (2.14)$$

2.2.2. Net charge determined using donor level statistics. At temperatures higher than the freeze-out temperature the population of all donor levels can be obtained in terms of the chemical potential, μ_d, using the grand canonical formalism. Consider a system of N donors, where each donor can be in one of m available states (these are the different DX-like and shallow states). Let $N_1, \ldots, N_m$ be the occupation numbers of each state ($N = N_1 + \ldots + N_m$), with l_i being the number of electrons trapped by a donor at state i, and ε_i is the energy of this donor state ($i = 1, \ldots, m$). The

grand canonical partition function of the donor system, *neglecting* mutual interactions among donors, is given by [29]

$$\mathcal{L} = \left(\sum_{i=1}^{m} \exp[\beta(\mu_d l_i - \varepsilon_i)] \right)^N .$$

The average occupation of each level, in thermal equilibrium, is given by [29]

$$N_j = -\frac{1}{\beta}\frac{\partial}{\partial \varepsilon_j} \ln \mathcal{L} = N \frac{\exp[\beta(\mu_d l_j - \varepsilon_j)]}{\sum_i \exp[\beta(\mu_d l_i - \varepsilon_i)]}. \quad (2.15)$$

Note that the coupling between the donor system and the lattice vibrations is not explicitly used, hence the energies ε_i should be interpreted as 'effective' energies (which might depend on temperature). Below the freeze-out temperature the frozen population of the DX levels is independent of μ_d. Thus, the population of the other, non-DX, active levels can also be described by equation (2.15) with N being replaced by the number of non-DX donors, the DX levels being omitted from the sum in the denominator.

The 2D charge density in the donor layer, ρ_0, for different thermal cycles can be found from the frozen population of the DX levels. Let us consider the two possible DX models: the DX^0 model, where the DX ground state is neutral, and the DX^- model, where the ground state is negatively charged (with an extra electron). For simplicity we assume a unique DX configuration with a single energy level, and we neglect the degeneracy of the donor states, i.e. the spin degeneracy of the d^0 state and the vibrational degeneracy of DX^- state. In both models the donors can also be either in a d^+ state or in a d^0 state. Thus, in both models, all non-DX donors are positively charged in the linear regimes seen in figure 2. In these regimes, assuming a DX^0 model, only the shallow donors contribute to the net charge density in the donor layer, which is given by $\rho_0 L^2 = e(N - N_{DX^0})$; hence by equation (2.15) one obtains

$$\frac{\rho_0}{en_0} = 1 - \frac{\exp[\beta_f(\mu_d - \varepsilon_{DX^0})]}{1 + \exp[\beta_f(\mu_d - \varepsilon_{d^0})] + \exp[\beta_f(\mu_d - \varepsilon_{DX^0})]} \quad (2.16)$$

where $\beta_f = 1/k_B T_f$. For the DX^- model, however, the frozen population of DX^- donors also contributes to the net charge density in the donor layer, $\rho_0 L^2 = e(N - 2N_{DX^-})$; hence by equation (2.15) one obtains

$$\frac{\rho_0}{en_0} = 1 - \frac{2\exp[\beta_f(2\mu_d - \varepsilon_{DX^-})]}{1 + \exp[\beta_f(\mu_d - \varepsilon_{d^0})] + \exp[\beta_f(2\mu_d - \varepsilon_{DX^-})]}. \quad (2.17)$$

Note that the chemical potential, μ_d, is calculated by equation (2.1) via the measured n_s at 160 K for each V_C.

2.2.3. Charge state of the DX centres. We now compare the values of ρ_0 obtained by solving the Poisson equation, equation (2.13), with those obtained by the grand canonical formalism for either the DX^0 model (equation (2.16)), or the DX^- model (equation (2.17)).

Table 1. The frozen charge density in the δ-doping plane, ρ_0, obtained by the Poisson equation and by donor level statistics for the DX^- model.

	ρ_0/e (10^{12} cm^{-2})	
V_C (V)	Poisson, equation (2.13)	Statistics, DX^-, equation (2.17)
−1	3.5	3.5
−0.5	2.8	2.4
0	1.9	1.8
+0.5	1.2	1.3
+1	0.59	1.0

As seen in table 1 we find a reasonable agreement between the DX^- model and the Poisson equation, with a Schottky barrier height $V_s = 1$ V (the increased value of V_s is probably due to an oxide layer in the metal–semiconductor interface), $\varepsilon_{d^0} = 90$ meV (this value is taken from section 2.1), and the fitting parameter $\varepsilon_{DX^-} = 270$ meV (135 meV per electron). Note that the fitting parameter, ε_{DX^-}, is modified by no more than 5% when one also considers spin degeneracy of the d^0 state and a vibrational degeneracy of the DX^- state of order 2. For the DX^0 model, however, the two methods do not agree for any choice of the fitting parameters: ε_{d^0} and ε_{DX^0}, since equation (2.16) predicts a change in ρ_0/e by some 10^{12} cm^{-2} at most in the biasing range -1 V $\leqslant V_C \leqslant +1$ V, much too small compared with the change predicted by equation (2.13). Additional confirmation for the DX^- model is provided in section 3.1.

3. Scattering times of the 2DEG

In general, the transport properties of a 2DEG are characterized by the momentum relaxation time, τ_t, with the mobility $\mu = e\tau_t/m^*$, and the single-particle relaxation time, τ_s. Since these scattering times strongly depend on the spatial distribution of charges in the doping layer, transport measurements provide an important tool for studying the charge state of the DX centres and the correlation between charged donors.

3.1. Mobility and charge state of the DX level

The measured mobility as a function of the 2DEG density, n_s, in the linear regimes seen in figure 3 is plotted in figure 4(*a*) for various thermal cycles. The donor charge density, ρ_0, strongly depends on V_C, and is calculated, using equation (2.13), to be $\rho_0/e = 5.9\times10^{11}$, 1.9×10^{12} and 3.5×10^{12} cm^{-2} for $V_C = 1$ V, 0 V and -1 V, respectively (see also table 1). Even though ρ_0 changes by a factor of six for these three thermal cycles the mobility is found to be almost independent of ρ_0. This observation provides an important insight into the charge state of the DX donors. The DX^0 model, with only the shallow, positively charged d^+ donors contributing to scattering, would predict a substantial decrease in

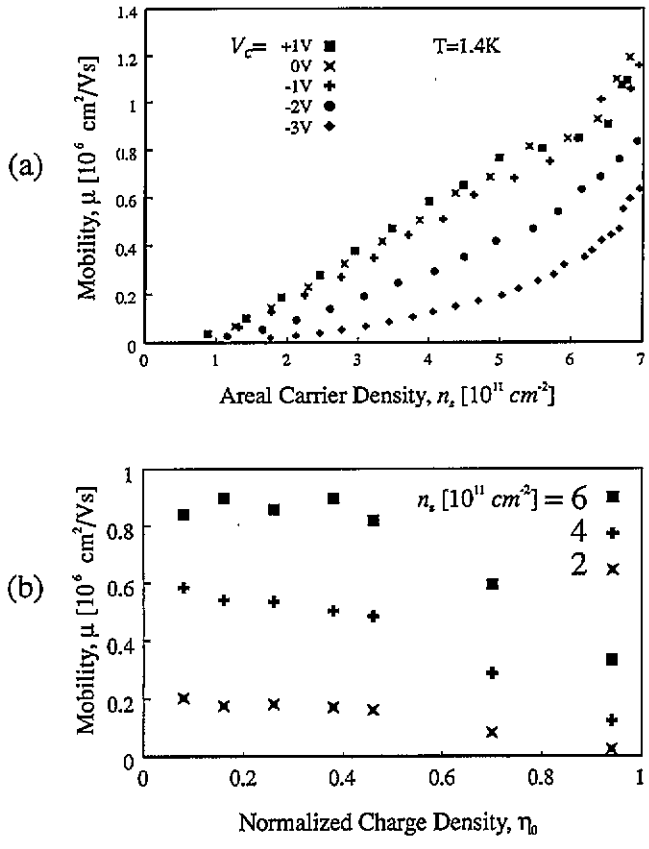

Figure 4. Mobility (*a*) versus areal carrier density of the 2DEG and (*b*) versus η_0 for the different thermal cycles. The mobility drops for $V_C < -1$ V or $\eta_0 > 0.5$. Note the onset of second subband transport for $n_s < 6 \times 10^{11}$ cm^{-2}.

the mobility with decreasing V_C, due to an increase in N_{d^+}. However, in the DX^- model the mobility of the 2DEG is affected both by the negatively charged DX^- centres and the positively charged d^+ donors (their sum is constant and is equal to the doping level). Thus, neglecting correlation effects, the mobility is expected to be insensitive to V_C over a large range of voltages. Our observation reconfirms and substantiates the DX^- model (see also section 2.2.3), and thus the negative-*U* model [23, 24].

3.2. Controlling correlation via thermal cycling

If indeed charge correlation was to set in, when would we expect it to be significant? Most likely when the number of possible internal arrangements of the charged donors system will be the highest. In other words when the number of occupied deep centres (DX^-) is similar to the number of empty shallow donors (d^+). It is convenient to define by η_0 the ratio between the net charge and the total number of charges, $\eta_0 = (N_{d^+} - N_{DX^-})/N$, with extreme values of 1 or -1. In principle, the first, $\eta_0 = 1$, when all donors are d^+-like, is realized with thermal cycles under very negative V_C and applied V_G in the linear regimes seen in figure 2; while the other extreme, $\eta_0 = -1$, when all donors are DX^--like, can in principle be approached with thermal cycles under extremely positive V_C. In both extreme

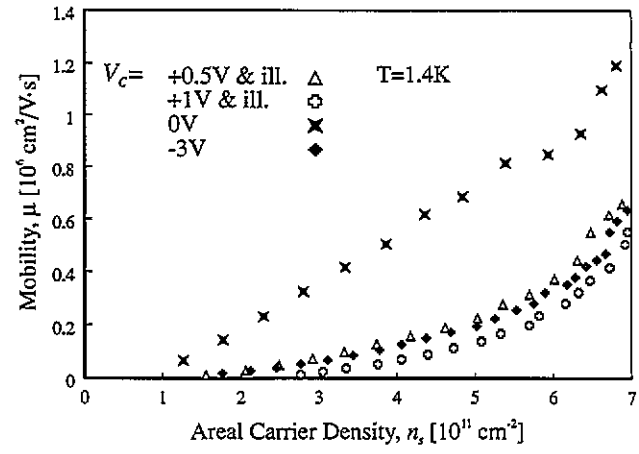

Figure 5. The measured mobility versus areal carrier density for thermal cycles followed by illumination. The results for the thermal cycles with $V_C = 0$ V and $V_C = -3$ V are also given fr comparison.

cases, when all donors are of the same kind, we do not expect any correlation between the charged donors due to their random positions in the lattice†. How far from these extremes are we? In practice one can reach only the regime where $0 < \eta_0 < 1$ due, in part, to an onset of leakage currents through the gate at large V_G. The regime where $\eta_0 < 1$ is not accessible due also to an unrealistic solution of the Poisson equation. The actual value for η_0 can be calculated from the net charge in the doping layer, given by equation (2.13), and the nominal doping level, being in our structure $n_0 = 7.5 \times 10^{12}$ cm^{-2}. In the widest possible range of cooling voltages (without gate leakage current), $V_C = -3, -2, -1, 0, +1$ V, we calculate $\eta_0 = 0.94, 0.70, 0.46, 0.26, 0.08$ respectively, and thus expect the correlation among charged donors to diminish for $\eta_0 \to 1$, namely for sufficiently negative V_Cs. This is indeed observed in the mobility drop seen in figure 4(*a*) (for $V_C \leqslant -2$ V), and also in figure 4(*b*), where we plot the mobility versus η_0 for three different values of n_s. Since the total number of charged ions is fixed in all thermal cycles, and is equal to N, the strong observed effect on the mobility can be attributed only to correlation between the charged donors setting in or being destroyed.

3.3. Controlling correlation via illumination

Photoexcitation of electrons out of the DX^- centres can be quite effective in destroying correlation among charged donors [18]. Being a spatially random process photoexcitation is expected to eliminate DX^- centres and randomly create persistent d^+ (or d^0) centres, thus reducing correlation that sets in and freezes at T_f. To explore this effect, the thermal cycles with $V_C = +0.5$ V and $+1$ V were followed by controlled illumination with a sequence of short pulses applied by an IR light emitting diode at $V_G = 0$. The process continued until the density

† The distribution of Si sites is not totally random; however, the effect on the mobility due to these kinds of correlation is negligibly small compared with the effect of Coulomb-originated correlation.

of the 2DEG was restored to the same value as in the thermal cycle with $V_C = 0$ V, implying the same ρ_0 ($V_C = 0$ V) but with a more randomized configuration. The measured mobility, seen for both cases in figure 5, is considerably smaller, indicating destruction of the correlation. For comparison the mobility is also plotted for the case of $V_C = 0$ V (correlated) and $V_C = -3$ V (uncorrelated) cases. We stress again that all mobilities, measured at the same temperature, same gate voltage and same n_s, are lower by up to a factor of six from that measured after the thermal cycle with $V_C = 0$ V. Note that a more dramatic effect is found when illumination follows the thermal cycle with $V_C = +1$ V (versus $V_C = +0.5$ V). This is a direct result of the longer illumination needed to restore n_s to its value for $V_C = V_G = 0$ V, and thus the higher randomization of charges that is taking place.

3.4. Comparison with other samples

To further substantiate our results we have fabricated and measured samples with the same AlAs mole fraction but with a lower donor concentration. In general, the comparison between different samples is relatively unreliable since the mobility strongly depends on the spacer width, which in turn is not reproducible to the desired accuracy. Hence, we compared the relative reduction in the mobility, as correlation diminished, for each sample separately. We found for samples with $n_0 = 7.5\times10^{12}$, 2.5×10^{12}, 1.0×10^{12} and 6.0×10^{11} cm^{-2}, mobility reduction of up to a factor of 6, 1.8, 1.4 and 1.3 respectively. This behaviour is expected since in the lower doping samples the Coulombic interactions are weaker and so is the correlation among the donors. Moreover, since the minimum number of d^+ centres is n_s it is more difficult to have low η_0 when N approaches n_s.

4. Theory

The mobility of the electrons in the 2DEG is limited by potential fluctuations $\delta\phi(r)$ created in the plane of the 2DEG by impurity charge density fluctuations $\delta\rho(r)$ in the δ-doping layer (the average charge density and the average potential do not contribute to scattering [10]).

Two types of charge density fluctuations exist. The first are fluctuations in the distribution of the impurity sites (impurity configuration). These fluctuations are defined by the crystal growth conditions and are 'frozen' at the growth temperature, about 900 K. The second are fluctuations of the charge state of a given impurity, which can be positive or negative. These fluctuations are defined by the 'freezing' of the impurity metastable DX states which occurs around 130 K. A procedure which resembles averaging over these fluctuations was considered by Ridley under the name statistical screening [12]. Averaging over the fluctuations of the charge state of a given impurity was considered by Efros *et al* [8] (for the positive-U model, when the impurity can be neutral or positive). Our aim is to present a theory that takes into account both types of fluctuations and their interaction (for the case of the negative-U model).

The scattering rate of the electron from state k to state k' is given by the Fermi golden rule

$$W_{k\to k'} = \frac{2\pi}{\hbar}\frac{e^2}{L^2}\delta(E_k - E_{k'})\frac{1}{L^2}|\delta\phi_q|^2. \tag{4.1}$$

Here L^2 is the area of the 2DEG and that of the δ-doping layer, $q = |k - k'|$, E_k is the electron energy, $\delta\phi_q$ is the qth Fourier component of the potential fluctuations $\delta\phi(r)$

$$\delta\phi(r) = \int \mathrm{d}^2q \exp(\mathrm{i}qr)\delta\phi_q. \tag{4.2}$$

The potential fluctuations in the 2DEG plane are related to the charge density fluctuations in the δ-doping plane

$$\delta\phi(r) = \int \mathrm{d}^2r\, V(r - r')\delta\rho(r') \tag{4.3}$$

or in terms of the Fourier components

$$\delta\phi_q = \delta\rho_q V_q \tag{4.4}$$

where $V(r - r')$ is the potential created at the point r of the 2DEG plane by a charge $+1$ at the point r' of the δ-doping plane. This potential V takes into account screening by the 2DEG and other charges, for example in a metal gate, if such exist. Assuming that the impurity potential is screened only by the 2DEG one has

$$V_q = \frac{\exp(-dq)}{2\varepsilon\varepsilon_0(q + q_s)} \tag{4.5}$$

where d is the spacer width, $\varepsilon = (\varepsilon_1 + \varepsilon_2)/2$, $q_s = 2/a_B$ is the screening wavevector and a_B the Bohr radius, calculated using ε.

Using equation (4.4) in equation (4.1) leads to

$$W_{k\to k'} = \frac{2\pi}{\hbar}\frac{e^2}{L^2}\delta(E_k - E_{k'})|V_q|^2\frac{1}{L^2}|\delta\rho_q|^2. \tag{4.6}$$

Neglecting mesoscopic effects one can replace $|\delta\rho_q|^2$ by its average over both types of charge fluctuations. To describe these fluctuations we will use a continuous model, namely, only large-scale fluctuations are important in electron scattering. This means that the distance between the impurities in the δ-doping plane, $n_0^{-1/2}$, is much smaller than the size of the fluctuation corresponding to the relevant q^{-1}.

From equations (4.5) and (4.6) one can see that only fluctuations with $q \leqslant 1/d$ are important in electron scattering. On the other hand, from momentum conservation it follows that $q < 2k_F$. As a result one can see that the continuous model is valid if $n_0^{-1/2} \ll \max[d, \lambda_F]$, where λ_F is the Fermi wavelength.

In the continuous model the impurity density and the charge of a given impurity are smooth random functions $n(r)$ and $e\eta(r)$, defined as averages of the corresponding

discrete ones. Thus the charge density in the continuous model is

$$\rho(r) = en(r)\eta(r) \tag{4.7}$$

where we represent

$$n(r) = n_0 + \delta n(r) \tag{4.8}$$

with n_0 being the average impurity density. With this definition

$$\langle \delta n(r) \rangle = 0 \tag{4.9}$$

where $\langle\rangle$ means configurational averaging. We also represent

$$\eta(r) = \eta_0 + \delta\eta(r) \tag{4.10}$$

where η_0 is the average charge of an impurity in the case when the impurity distribution is homogeneous with density n_0. Note that with this definition of $\delta\eta$

$$\overline{\delta\eta(r)} \neq 0 \tag{4.11}$$

where the over bar means averaging over thermodynamic fluctuations of the charge state of a given impurity for a fixed impurity configuration. This is because the fluctuations of η are on top of an inhomogeneous impurity distribution that determines the non-zero average. Due to the inhomogeneous impurity distribution an average potential $\overline{\psi(r)}$ appears in the δ-doping plane. This potential changes the average impurity charge $\overline{\eta(r)}$. The corresponding charge density $\overline{\delta\rho(r)}$ is consistent with the potential $\overline{\psi(r)}$ through the Poisson equation with the screened interaction $Q(r-r')$ (see equation (4.16)).

Assuming small fluctuations of η, the charge density is

$$\rho(r) = \rho_0 + \delta\rho(r) \tag{4.12}$$

with

$$\rho_0 = en_0\eta_0 \tag{4.13}$$

and

$$\delta\rho(r) = en_0\delta\eta(r) + e\eta_0\delta n(r). \tag{4.14}$$

We now calculate the fluctuations $\langle\overline{|\delta\rho_q|^2}\rangle$ as follows. First we average over the fluctuations of $\eta(r)$ for a given $n(r)$ and then we average over $n(r)$.

To perform the average over the impurity charge state we use the 'non-equilibrium' model of Efros *et al* [8], assuming that the fluctuations $\delta\eta$ are equilibrium fluctuations corresponding to the 'freeze-out' temperature $T = T_f$. Since we are interested in long-range fluctuations, these fluctuations are macroscopic (many impurities participate in each fluctuation).

According to the general theory of fluctuations [29] the probability $P\{\delta\eta\}$ of finding a given fluctuation $\delta\eta$ is proportional to $\exp(-\delta F\{\delta\eta(r)\}/k_BT)$, where δF is the change in free energy due to the fluctuation $\delta\eta$. We have $\delta F = \delta E - T\delta S$, where δE and δS are the corresponding changes in energy and entropy.

The change in entropy can be represented as

$$\delta S = -\frac{1}{2}\int d^2r\, n(r)\frac{\delta\eta(r)^2}{(\delta\eta^2)_0} \tag{4.15}$$

where $(\delta\eta^2)_0$ is the average fluctuation for an isolated single impurity. It depends on temperature and external potentials.

The change of energy in our case is the change in Coulomb energy due to the change in charge density $\delta\rho(r)$

$$\delta E = \frac{1}{2}\int d^2r\, d^2r' Q(r-r')\delta\rho(r)\delta\rho(r') \tag{4.16}$$

where $Q(r-r')$ is the Coulomb interaction between two charges $+1$ in the δ-doping plane located at r and r'. This interaction is screened by the same charges that screen the potential $V(r-r')$. For example, when the electrons in the 2DEG are the only screening charges

$$Q_q = \frac{1}{2\varepsilon_2\varepsilon_0 q}[1 + \sigma_q \exp(-2dq)] \tag{4.17}$$

where

$$\sigma_q = \frac{(\varepsilon_2 - \varepsilon_1)/(\varepsilon_2 + \varepsilon_1) - q_s/q}{1 + q_s/q}. \tag{4.18}$$

When $q \ll q_s$ the 2DEG screens as a perfect metal plane and we obtain the interaction used in [8]

$$Q_q = \frac{1}{2\varepsilon_2\varepsilon_0 q}[1 - \exp(-2dq)]. \tag{4.19}$$

Neglecting higher-order terms one can put $n(r) = n_0$ in δS, leading to

$$\frac{\delta F}{k_BT} = \frac{n_0}{2(\delta\eta^2)_0}\int d^2r\,\delta\eta(r)^2 + \frac{1}{2k_BT}\int d^2r\, d^2r' Q(r-r')\delta\rho(r)\delta\rho(r'). \tag{4.20}$$

Since δF is now translation invariant, and we can represent it in terms of the Fourier transform

$$\delta F = \int \frac{d^2q}{(2\pi)^2}\delta F_q \tag{4.21}$$

where

$$\frac{\delta F_q}{k_BT} = \frac{n_0}{2(\delta\eta^2)_0}|\delta\eta_q|^2 + \frac{1}{2k_BT}Q_q|\delta\rho_q|^2 \tag{4.22}$$

with

$$\delta\rho_q = en_0\delta\eta_q + e\eta_0\delta n_q. \tag{4.23}$$

One can see now that δF_q is quadratic in $\delta\eta_q$, i.e. δF_q is a Gaussian functional. To consider the Fourier components as Gaussian variables it is convenient to change from integration in equation (4.21) to summation and write

$$\delta F = \frac{2}{L^2}\sum_q{}' \delta F_q \tag{4.24}$$

where the sum with the prime means that we count only half of all the values of q, since the fluctuating quantities are real and the Fourier components with q and $-q$ are

complex conjugate. The factor 2 appears due to this counting.

Since δF does not contain cross terms with different qs, Fourier components $\delta\eta_q$ with different qs are uncorrelated. For the same reason the real and imaginary parts of each component are also uncorrelated. Having this in mind one can easily calculate the average

$$\overline{\delta\eta_q} = -\frac{\eta_0}{n_0}\frac{u_q}{1+u_q}\delta n_q \tag{4.25}$$

and

$$\overline{|\delta\eta_q|^2} - |\overline{\delta\eta_q}|^2 = \frac{L^2}{n_0}\frac{(\delta\eta^2)_0}{1+u_q} \tag{4.26}$$

where we define

$$u_q = (\delta\eta^2)_0\frac{n_0e^2}{k_BT_f}Q_q. \tag{4.27}$$

Equation (4.25) represents the above-mentioned interaction between both types of fluctuations: configurational fluctuations δn shift the average of the impurity charge state fluctuations $\delta\eta$.

With the averages in equations (4.25) and (4.26) one finds

$$\overline{|\delta\rho_q|^2} = e^2n_0L^2\frac{(\delta\eta^2)_0}{1+u_q} + \frac{e^2\eta_0^2}{(1+u_q)^2}|\delta n_q|^2. \tag{4.28}$$

To perform the last average over the fluctuations of $n(r)$ let us define the correlator

$$\langle\delta n(r)\delta n(r')\rangle = n_0[\delta(r-r') + g(r)] \tag{4.29}$$

where $g(r) \equiv 0$ if the impurity density fluctuations are uncorrelated. From these definitions it follows that

$$\langle|\delta n_q|^2\rangle = L^2n_0(1+g_q). \tag{4.30}$$

Using equation (4.30) in equation (4.28) leads finally to

$$\langle\overline{|\delta\rho_q|^2}\rangle = e^2n_0L^2\left(\frac{(\delta\eta^2)_0}{1+u_q} + \frac{\eta_0^2}{(1+u_q)^2}(1+g_q)\right). \tag{4.31}$$

The first term appears due to the fluctuations of the charge state of a given impurity while the second is due to the fluctuations of the impurity density.

We now find a relation between η_0 and $(\delta\eta^2)_0$. The impurity can be in two different states: $1 = d^+$ and $2 = DX^-$ with probabilities w_1 and w_2. Using these probabilities one can calculate

$$\eta_0 = \bar{\eta} = w_1 - w_2 \tag{4.32}$$

and

$$\bar{\eta^2} = w_1 + w_2 = 1. \tag{4.33}$$

It follows from these equations that

$$(\delta\eta^2)_0 = 1 - \eta_0^2. \tag{4.34}$$

Returning to the scattering rate we assume that the impurity distribution is uncorrelated, namely $g_q = 0$. Using equation (4.34) we find a more explicit expression for charge correlations

$$\langle\overline{|\delta\rho_q|^2}\rangle = e^2n_0L^2\chi(\xi, \nu_q) \tag{4.35}$$

where the correlator factor is

$$\chi(\xi, \nu_q) = \frac{1+\nu_q\xi^2}{(1+\nu_q\xi)^2} \tag{4.36}$$

with

$$\nu_q = \frac{n_0e^2}{k_BT_f}Q_q \tag{4.37}$$

and

$$\xi = (\delta\eta^2)_0 = 1 - \eta_0^2. \tag{4.38}$$

The correlation effects disappear, i.e. $\chi = 1$, in two cases:

(i) All the impurities are in the same charge state, $\eta_0 = \pm 1$, thus there are no fluctuations in the impurity charge state, i.e. $\xi = 0$.

(ii) The screened Coulomb interaction between two charges in the δ-doping plane at distance d is weak compared with the freeze-out temperature, i.e. $\nu_q \ll 1$ for $q \simeq d^{-1}$.

Finally we arrive at the electron scattering times, using equations (4.6) and (4.35) the momentum relaxation time is

$$\frac{1}{\tau_t} = \frac{2\pi n_0e^4}{\hbar}\int\frac{d^2q}{(2\pi)^2}\delta(E_{k_F} - E_{k_F+q})|V_q|^2 \times \chi(\xi, \nu_q)F(q)(1-\cos\theta) \tag{4.39}$$

where θ is the scattering angle between k_F and $k_F + q$. The form factor, $F(q)$, is introduced in order to account for the final width of the electronic wavefunction. It is estimated by the Fang–Howard approximation [1]

$$F(q) = \left(\frac{b}{b+q}\right)^3 \tag{4.40}$$

where

$$b = \left[\frac{12m^*e^2}{\varepsilon\varepsilon_0\hbar^2}\left(\frac{11}{32}n_s + n_{depl}\right)\right]^{1/3}. \tag{4.41}$$

Here, as in section 2.1, we neglect the depletion charge. Note that the single-particle scattering time, τ_s, is given by omitting the term $(1-\cos\theta)$ from equation (4.39).

5. Discussion and summary

Our theory, developed for a continuous model (where fluctuation on the scale of the interatomic distances are averaged out), where the only relevant potential fluctuations are with a length scale of the order or greater than the spacer d, leads to a reasonable agreement

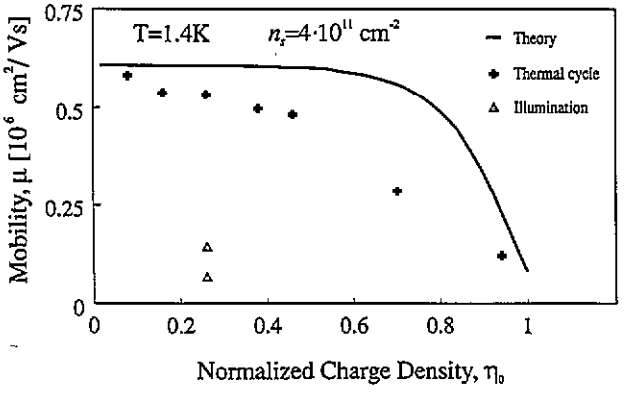

Figure 6. Calculated and measured mobility versus η_0 for $n_s = 4 \times 10^{11}$ cm^{-2}. The full curve is calculated with $T_f = 130$ K and $d = 9$ nm.

with experiment. We plot in figure 6 the calculated and measured mobility versus η_0 (normalized charge density in the δ-doping plane) for a 2DEG density $n_s = 4 \times 10^{11}$ cm^{-2}. The full curve that summarizes the theoretical results is calculated with $T_f = 130$ K and $d = 90$ nm (to account for some charge spreading due to diffusion of the Si in the δ-doping plane). Noting that the experimental and theoretical results agree reasonably well, not only in general behaviour but also in absolute values, gives some confidence in the theory. The presented theory reduces to the standard uncorrelated one when we assume no correlation ($v_q = 0$ or $\eta_0 = \pm 1$). For comparison we add the measured mobilities for two thermal cycles followed by illumination. These results agree with the uncorrelated mobility as seen in figure 6 for $\eta_0 = 1$.

As was also pointed out before, the mobility is quite insensitive to η_0 for small η_0, where correlation is strong. For $\eta_0 > 0.5$ the mobility drops precipitously indicating onset of random scattering (see figure 4(*b*)). As observed, the theoretical results predict a sharper transition from 'ordered' to 'disordered' potential, most probably due to the averaging process we adopt by utilizing the continuous model.

We also measured the single-particle relaxation time as a function of the density of the 2DEG after each thermal cycle. The determination of τ_s is based on the measured amplitude of the SdH oscillations as a function of magnetic field, which is fitted with the predicted behaviour of the magnetoresistance by the theory of Laikhtman and Altshuler [3]. We had difficulties in determining τ_s due to the resultant nonlinear Dingle plots [9] that could not be extrapolated to zero. Hence, the determined scattering times deviated strongly from sample to sample and were unreliable.

A further test of our conclusions could be performed if a different dopand (rather than Si) could be introduced with a different freeze-out temperature T_f. Since T_f is the most important single parameter determining the extent of correlation, a lower T_f could affect the mobility drastically. In the absence of a known donor with lower T_f in AlGaAs [14], we have also grown heterostructure with a pure AlAs as a barrier. It is expected that the DX level is degenerate again with the conduction band

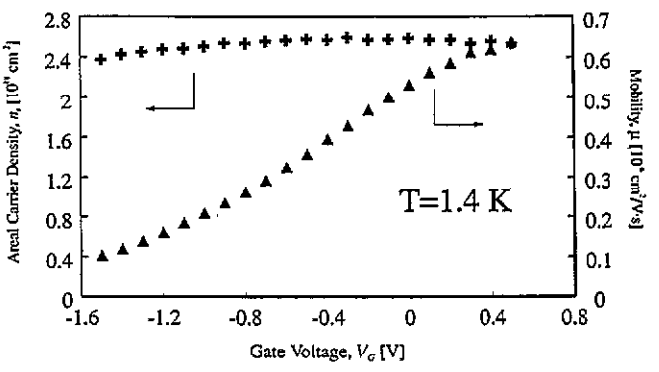

Figure 7. Areal carrier density and mobility versus gate voltage for GaAs–AlAs heterostructure.

and the deepest donor is an active donor with a very low (if at all) freeze-out temperature. Indeed freeze-out effects in the GaAs–AlAs heterostructure were not observed. Figure 7 displays the measurements of n_s and μ versus gate voltage. Unfortunately, due to too high a doping concentration in the δ-doping plane ($n_0 = 2.5 \times 10^{12}$ cm^{-2}) we have not succeeded in fully depleting the δ-doping plane, as seen from the almost saturated n_s in figure 7. Hence, the remarkable increase in the mobility with increasing gate voltage can be mostly accounted for by the reduction in the number of charged impurities in the δ-doping plane. The consistently higher mobility we get in the 2DEG supported by GaAs–AlAs heterostructures suggests that the low T_f and the resulting correlation plays an important role, but this is still open for future investigations.

In summary, we have given conclusive evidence for the existence of correlation among positively and negatively charged donors coexisting in the donor supply layer of selectively doped GaAs–AlGaAs heterostructures supporting two-dimensional electron gases (2DEG). This was done by first demonstrating that the donors can be either metastable DX-like or shallow donors, agreeing with the negative-U model. A strong enhancement in the mobility was observed when correlation among the charged donors sets in. The effects we measured are dramatic, and it is amazing why so little attention has been devoted to this so far. We tend to suspect that such an effect is quite prevalent in many doped semiconducting systems not yet studied in detail. We present here a theory for correlation among positive and negative charges in the δ-doping layer that seems to account approximately for the enhancement in the measured mobilities.

Acknowledgments

This work was partly supported by the Ministry of Defence (contract #7036) and the Bosch Foundation (grant #5630). One of the authors (YL) would like to acknowledge M Pollak, D Khmelnicki and A Larkin.

References

[1] Ando T, Fowler A B and Stern F 1982 *Rev. Mod. Phys.* 54 437

[2] Mendez E E 1986 *IEEE J. Quantum Electron.* 22 1720

[3] Laikhtman B and Altshuler E L 1994 *Ann. Phys., NY* **232** 332
[4] Ando T 1982 *J. Phys. Soc. Japan* **51** 3900
[5] Ablyazov N N and Efros A L 1989 *Zh. Eksp. Theor. Fiz.* **95** 1450
[6] Lassing R 1988 *Solid State Commun.* **65** 765
[7] Efros L 1988 *Solid State Commun.* **65** 1281
[8] Efros A L, Pikus F G and Samsonidze G G 1990 *Phys. Rev.* B **41** 8295
[9] Coleridge P T 1991 *Phys. Rev.* B **44** 3793
[10] Van Hall J 1989 *Superlatt. Microstruct.* **6** 213
[11] Van Hall P J, Klaver T and Wolter J H 1988 *Semicond. Sci. Technol.* **3** 120
[12] Ridley B K 1987 *Semicond. Sci. Technol.* **3** 111
[13] Sobkowicz P, Wilamowski Z and Kossut J 1992 *Semicond. Sci. Technol.* **7** 1155
[14] Suski T *et al* 1994 *Solid State Electron.* **37** 801
[15] Mycielski J 1986 *Solid State Commun.* **60** 165
[16] Monroe D 1991 *Appl. Phys. Lett.* **59** 2293
[17] O'Reilly E P 1989 *Appl. Phys. Lett.* **55** 1409
[18] Coz P L, Ghezzi C and Parisini A 1993 *Semicond. Sci. Technol.* **8** 13
[19] Maude D K 1992 *Appl. Phys. Lett.* **60** 1993
[20] Van Der Wel P J *et al* 1993 *Semicond. Sci. Technol.* **8** 211
[21] Wilamowski Z *et al* 1991 *Semicond. Sci. Technol.* **6** B 34
[22] Dmowski L H *et al* 1993 *Japan. J. Appl. Phys.* **32** 221
[23] Chadi D J and Chang K J 1988 *Phys. Rev. Lett.* **61** 873
[24] Chadi D J and Chang K J 1989 *Phys. Rev.* B **39** 10063
[25] Makinen J *et al* 1993 *Phys. Rev. Lett.* **71** 3154
[26] Mooney P M 1990 *J. Appl. Phys.* **67** R1
[27] Schubert E F 1990 *J. Vac. Sci. Technol.* A **8** 2980
Kohler K, Ganser P and Maier M 1993 *J. Crystal Growth* **127** 720
[28] Rooks M J *et al* 1991 *J. Vac. Sci. Technol.* B **9** 2858
[29] Pathria R K 1972 *Statistical Mechanics* (Oxford: Pergamon)